Tectonophysics 667 (2016) 1–15

Contents lists available at ScienceDirect

Tectonophysics

journal homepage: www.elsevier.com/locate/tecto

Review Article

Anomalous values of gravity and magnetism in the western margin of Gondwana

Cecilia Weidmann *, Mario Gimenez, Federico Lince Klinger, Orlando Alvarez

Consejo Nacional de Investigaciones Científicas y Técnicas — CONICET, Argentina
Instituto Geofísico Sismológico Volponi, Universidad Nacional De San Juan, Argentina

ARTICLE INFO

Article history:
Received 13 February 2015
Received in revised form 14 November 2015
Accepted 20 November 2015
Available online 11 December 2015

Keywords:
Western Gondwana
Famatinian arc
Potential field methods
Western Sierras Pampeanas

ABSTRACT

This research is based on a joint geological and geophysical study performed in the South Central Andes region. We acquired and processed terrestrial and satellite gravity data, as well as terrestrial and aeromagnetic data. Balanced geological cross-sections were constrained by physical properties of rocks (densities and magnetic susceptibilities obtained from field samples and well log). This study was performed in order to interpret a complex region that is still under debate: the location of Famatinian magmatic arc and its boundary with the Cuyania terrain. By means of gravity anomaly we developed direct and inverse models constrained by field data. The existence of a major high-density geological structure was evidenced from these models, located below the Vinchina basin and to the east of Cerro Rajado respectively. The existence of such gravity high could be linked to the boundary between the Famatinian magmatic arc and the accreted Cuyania wedge.

Contents

1. Introduction . . . 2
2. Tectonic setting . . . 2
3. Geological aspects . . . 2
   3.1. Sierras Pampeanas . . . 2
   3.2. Famatina . . . 2
   3.3. Precordillera . . . 3
4. Terrestrial gravimetry . . . 4
   4.1. Methodology . . . 4
   4.2. Results . . . 4
5. Satellite gravimetry and vertical gravity gradient . . . 5
   5.1. Methodology . . . 5
   5.2. Results . . . 6
6. Aeromagnetometry . . . 6
   6.1. Methodology . . . 6
   6.2. Results . . . 7
   6.3. Reduction to pole of magnetic data . . . 7
      6.3.1. Methodology . . . 7
   6.4. Results . . . 7
7. Sampling of densities and magnetic susceptibilities . . . 7
8. 2D gravi-magnetometric direct models . . . 8
   8.1. Methodology . . . 8
   8.2. Results . . . 10
9. Inverse modeling . . . 10
   9.1. Methodology . . . 10
   9.2. Results . . . 10
10. Discussion . . . 11

* Corresponding author at: IGSV Ruta 12, Km 17, Marquesado, Rivadavia, San Juan 0054 264 4945015, Argentina.
E-mail addresses: ceciweidmann@yahoo.com.ar (C. Weidmann), gimmario@gmail.com (M. Gimenez), flklinger@hotmail.com (F.L. Klinger), orlando_a_p@yahoo.com.ar (O. Alvarez).

http://dx.doi.org/10.1016/j.tecto.2015.11.017
0040-1951/

11. Conclusions . . . 13
Acknowledgments . . . 13
References . . . 13

1. Introduction

In the South Central Andes region between 28°S and 31°S, the Famatina magmatic arc developed between Cuyania and western Gondwana (Miller and Söllner, 2005; Pankhurst et al., 1998; Toselli et al., 1996). Diverse authors have related this arc to the occidental border of Gondwana, produced by the subduction of Cuyania terrane; (Dahlquist et al., 2005a,b, 2006; Pankhurst et al., 1998; Ramos et al., 1998; Rapela et al., 1998, 2001; Sims et al., 1998; Toselli et al., 1996). The collision between both terranes has been proposed by diverse authors e.g.: Ramos et al. (1984, 1986, 1996), Thomas and Astini (1996), Rapela et al. (2001), Pankhurst et al., 1998; based on the conspicuous outcrops (mafic and ultra-mafic rocks) to the West of the study zone (Villar, 2003; Fauqué and Villar, 2003). Nevertheless, it is difficult to estimate the exact location of the suture zone due to the lack of geological information reported in the area.

This research addresses the probably suture zone location and the Famatina magmatic arc by means of potential field methods: gravimetry and magnetometry. Previous geophysical studies identified other suture zones to the south of the study region by using potential field methods (Giménez et al., 2000; Martínez et al., 2003; Alvarez et al., 2012; among others). The 2D and 3D derived maps adjusted with balanced geological sections and densities extracted from a well allowed us to observe a probable lateral distribution of densities and magnetic susceptibilities in the basement of Vinchina basin.

2. Tectonic setting

There are several hypotheses about accretion of the different terranes, as is the case of Laurentia with an allochthonous origin (Dalla Salda et al., 1992; Dalziel et al., 1994). Cuyania terrane as a rift-separated from Laurentia continent that collided in the western margin of Gondwana in mid-Ordovician times (Cristofolini et al., 2014; Ramos, 2004; Ramos et al., 1998; Thomas and Astini, 2003) or in Silurian–Devonian times (Keller et al., 1998; Pankhurst et al., 1998; Rapela et al., 1998) (Fig. 1).

Aceñolaza and Toselli (1988), Baldis et al. (1989), Aceñolaza et al. (2002) and Finney et al. (2003) proposed the Cuyania terrane as para-autochthonous to Gondwana, located in the same latitudinal belt as Laurentia. Thus, they explained the carbonate platform and fossils found in Cuyania. Following this hypothesis Cuyania terrain migrated along a transform fault, located on the southern margin of Western Gondwana (present coordinates) in Mid-Ordovician times, to its actual position of the Famatinian magmatic belt in Devonian times (Finney, 2007).

Ramos et al. (1984, 1986) defined Cuyania as a micro-continental length of early Paleozoic age. This terrane derived from Laurentia continent (Ramos et al., 1998); which is in turn made up of two micro-terrains: Precordillera and Pie de Palo separated by a Mid-Proterozoic ophiolitic belt. The collision between the Cuyania proto-margin and western Gondwana began at Mid-Ordovician time. Afterward uplifting and deformation lasted until the early Devonian, while the last deformational events are associated with the coupling of Chilenia (Ramos et al., 1998). Evidence of mafic and ultra-mafic rocks were reported by Vujovich and Kay (1998) in the Pie de Palo range south of the mentioned suture, finding some scarcer evidence to the North in the Famatina System (Vujovich, 1992). In this region the Vinchina basin presents a thick sedimentary cover that could be masking the presence of these rocks (Ramos, 2004).

The Sierras Pampeanas of northwestern Argentina are comprised of abundant granitoid batholiths and meta-volcanic rocks (of Ordovician age) that jointly define the Famatinian magmatic arc. This magmatic arc developed in response to the eastward subduction of a paleo-Pacific oceanic plate (e.g., Miller and Söllner, 2005; Pankhurst et al., 1998; Toselli et al., 1996). Further to the south, the Famatinian magmatic arc is mostly buried beneath Quaternary sediments that can be delineated up to 39°S by means of aeromagnetic data (Chernicoff et al., 2010).

3. Geological aspects

We used two balanced geological sections performed by SEGEMAR Argentine Geological-Mining Service (SEGEMAR) (Fauqué et al., 2005), which are based on geological surface observations.

In A–A′ section at 29° 30′S (Fig. 3) we used a profile of approximately 170 km length, in the W–E direction. It begins at the eastern Precordillera, cutting across the Vinchina basin to its culmination at the Famatina System. We considered geological information available concerning the area of the Vinchina basin (Collo et al., 2011; Fauqué et al., 2005 and Ramos, 1970), which reported a sedimentary thickness ranging from 7 to 10 km. The Famatina System constitutes a region of structural overlap (Dávila and Astini, 2003b) composed by a folded thrust belt that involves basement levels.

Section B–B′ is located at 29° 45′S (Fig. 3) with an extension of approximately 170 km length, predominantly in the W–E direction. It begins in the Precordillera Oriental, crossing through the Guandacol basin (Fig. 2) passing over Cerro Rajado (Valle Fértil range). The structure of the Western Sierras Pampeanas was defined by González Bonorino (1950) as basement uplifts under a compressive regime, affected by listric faults (see Giménez et al., 2000; Introcaso et al., 2004; Martinez, 1997).

3.1. Sierras Pampeanas

This morpho-structural unit represents a series of outcrops that emerged during the Andean orogenesis and are part of a cratonic block defined as Pampia by Ramos et al. (1993) and Vujovich (1993), located in the central–northern region of Argentina. The outcrops are composed of a series of important mountain ranges, among which the most relevant for this study are identified as Espinal, Maz, Umango, Toro Negro and Valle Fértil ranges (Fig. 2).

The basement of the Sierras Pampeanas is mainly comprised of a sequence of igneous and metamorphic rocks. The main rocks are: granite, migmatite, gneisses, schists, phyllite, marble, calceous-silicate rocks, of lower Proterozoic–Paleozoic age (Caminos, 1979; De Alba, 1954; Furque, 1972; Toselli et al., 1986; Turner, 1964). This metamorphic basement was intruded by granitic rocks from Ordovician to Carboniferous times. This magmatic activity is linked with the Pampean and Famatinian events (Aceñolaza and Toselli, 1976; Larrovere et al., 2012; Pankhurst et al., 2000; Sato et al., 2003). Vujovich and Kay (1996a,b) recognized a metamorphic band in the Western Sierras Pampeanas, which were originated (to a lesser degree) from the protoliths of mafic and ultramafic rocks of Precambrian age.

3.2. Famatina

The Famatina System is located in the Central Andean foreland and extends approximately along 400 km in a N–S direction as it is

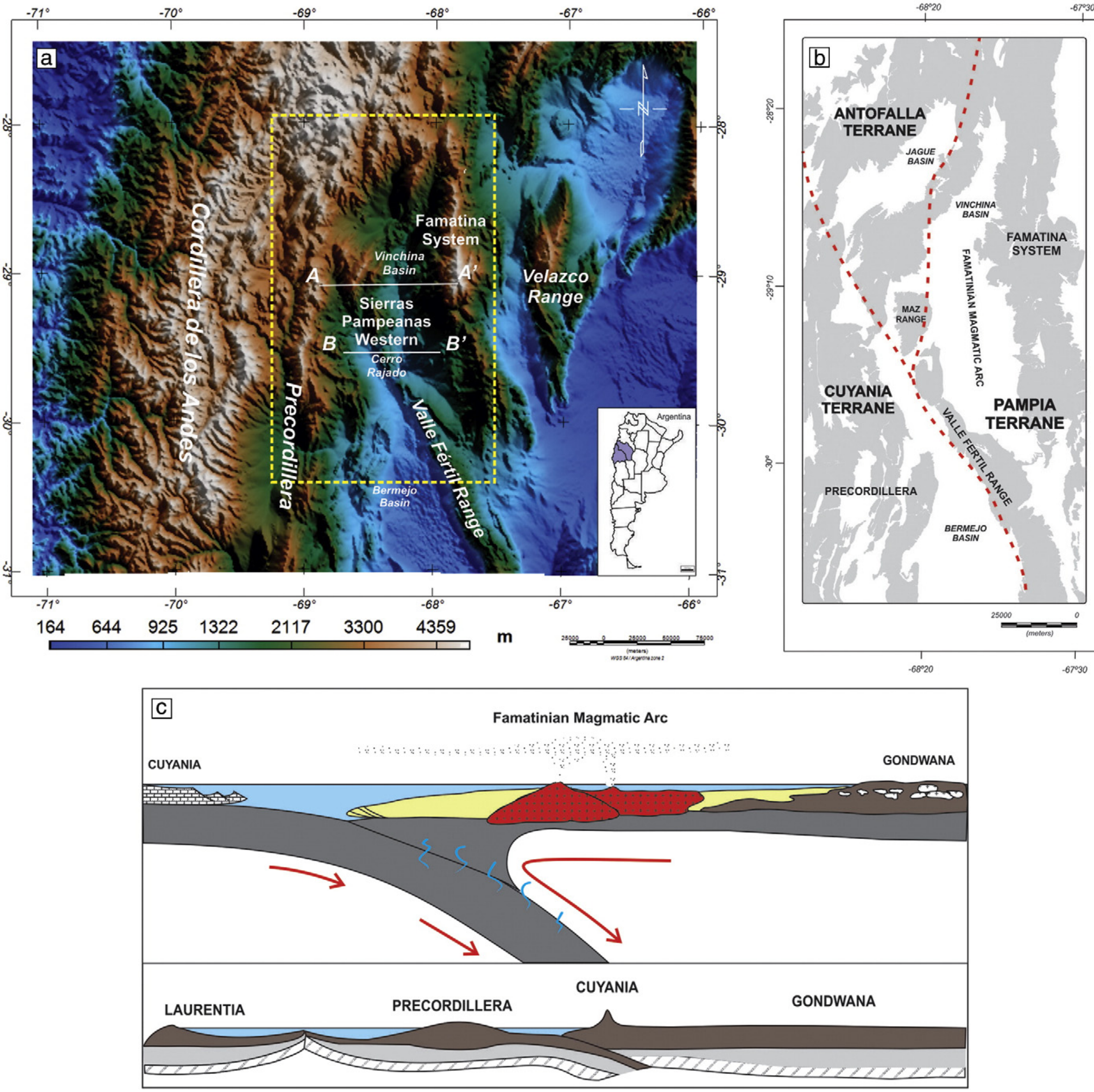

Fig. 1. a — location map represented by a digital elevation model (DEM) where it represented the study area by a yellow-shaded line, A–A′ and B–B′ indicate the location of the balanced geological sections that were modeled with gravity, cutting across the main intervening morpho-structural units. b — location of the different cratonic blocks and their relation with the adjacent blocks. c — schematic section of the tectonic setting, showing the relation between the terranes Cuyania, Godwana, & Laurentia and the location of the Famatina magmatic arc, at 500 Ma.
Modified by Ramos et al. (1996) and Cristofolini et al. (2014).

developed over the horizontal subduction segment of the Central Andes (Barazangi and Isacks, 1976) (Fig. 2). The Famatina System exhibits Paleozoic age stratigraphy, constituted by marine sequences. These sequences are associated with volcanic and metamorphic rocks, which are intruded by granitic, tonalities and monzogranite rocks related to the Famatinian orogenic cycle during the lower Paleozoic (Rapela et al., 2001 and references within). However, the Neo-Paleozoic sequences are represented by arkosic sandstones (Astini and Dávila, 2002; Bodenbender, 1922; Dávila and Astini, 2003a,b; De Alba, 1979; Turner, 1962) (Fig. 3).

3.3. Precordillera

The Jagüé Precordillera is located in a transition zone between the normal subduction and the low-angle subduction of the Central Andes (Allmendinger et al., 1982). This unit is mainly composed by Proterozoic and Paleozoic rocks, which lie below the Cenozoic vulcanites toward the North (where the geologic units of Precordillera, Famatina and la Puna converge) (Astini et al., 2011). The Ordovician stratigraphic sequence was determined by Caminos (1972) and is comprised of metagreywackes, phyllites, slate and marine limestone associated with

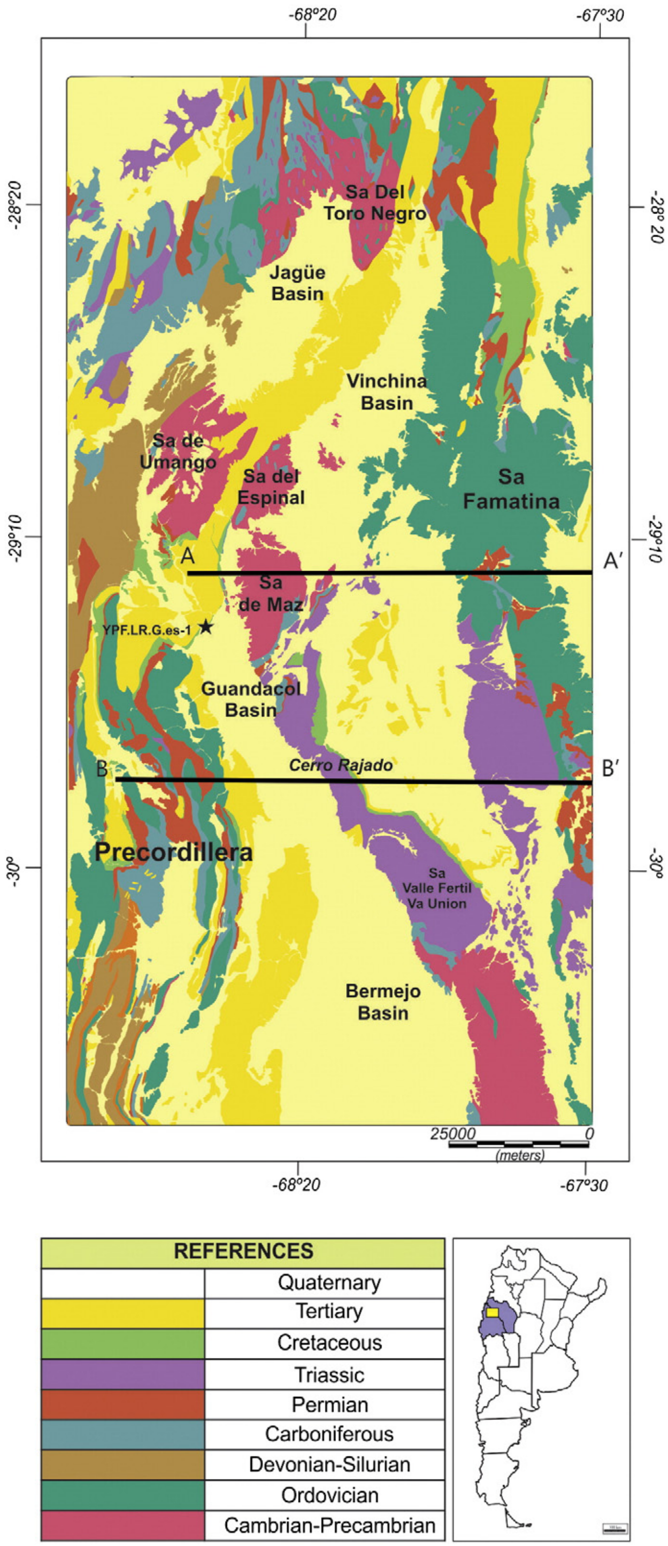

Fig. 2. Geologic map with the principal morpho-structural units of the area under study (Fauqué et al., 2005). Black lines indicate the location of both balanced cross sections: A–A′ and B–B′. The main morpho-structural units which cut through geological profiles are identified.

ophiolites (Villar, 2003). The Neo-Paleozoic sequence is evidenced by sediments containing plutonic intrusions of intermediate compositions and volcanic–sedimentary sequences (Aceñolaza et al., 1971; Caminos et al., 1993; Fauqué and Villar, 2003; Limarino and Cesari, 1992) (Fig. 2).

4. Terrestrial gravimetry

4.1. Methodology

For this study we used the gravity and magnetic anomalies database property of the Instituto Geofísico Sismológico Volponi (IGSV) of Universidad Nacional de San Juan (UNSJ). In addition, values taken from the Instituto Geográfico Nacional (IGN) during the 1980s (Fig. 4a) were used. These measurements are linked to the absolute value of gravity (97960.03 mGal) located at the Miguelete station, in Buenos Aires Province. The theoretical gravity was determined according to ellipsoid IGSN71 (International Gravity Standardization Net 1971) (Morelli et al., 1974), to be compatible with pre-existing values of the IGSV regional database.

Calculation of the Bouguer anomaly was performed using classic gravity expressions (Blakely, 1995). For the topographic correction, two digital elevation models (DEM) were used, obtained from the Shuttle Radar Topography Mission (SRTM): a) local DEM with a grid size of 90 m and b) regional DEM, which expanded 167 km outside of the local DEM, with a grid size of 250 m. Then, the value of the topographical correction was assigned to each gravimetric station. The corrected gravimetric anomaly values were regularized with a 2500 m separation distance by applying the minimum curvature method (Briggs, 1974).

The Bouguer anomaly map was computed using the grid parameters corresponding to the area of study (Fig. 4a). This map contains the sum of the regional and local gravimetric effects. The objective is to analyze the gravimetric response of geological structures located in the mid-to-upper crust. To achieve this, we applied filters based on the fast Fourier transform (FFT) algorithm, such as the upward continuation (Pacino and Introcaso, 1987; Blakely, 1995; among others). Following this methodology, we applied the upward continuation method up to 40 km over the geoid, obtaining the regional gravimetric effect. Filtering techniques in potential methods are widespread. The methods used for this work were tested by many authors such as Blakely (1995) and particularly in the study region by Fisher et al. (2002), Gimenez et al. (2009) and Götze and Krause (2002), among others. The residual Bouguer anomaly map was obtained by removing the regional gravimetric effect from the Bouguer anomaly map (Fig. 4a and b).

4.2. Results

The Bouguer anomaly map (Fig. 4a) ranges approx. between −400 to +180 mGal. This map contains the effect of important geological structures, such as the Andean roots, the Precordillera, the Sierras Pampeanas, the Famatina System and sedimentary basins in the center and east of the map. Minimum negative values are due to the effect produced by the Andean roots, while the maximum positive observed is linked to the Valle Fértil range. In this map (Fig. 4a), and in the Bouguer residual anomaly map (Fig. 4b), positive anomaly values can be highlighted, in agreement with the location of the geological structures that exhibit higher density values than the reference considered in the Bouguer correction (2.67 g/cm^3). This can be observed in the Valle Fértil and Maz ranges which are mainly composed by high-density metamorphic rocks (Cristofolini et al., 2014; Zaffarana et al., 2011). On the contrary, negative values are associated with low-density geological structures, as sedimentary basins of Bermejo, Pagancillo, Guandacol and North of Vinchina. Nevertheless, the southern sector of the Vinchina basin and West of Famatina presents positive gravity values.

The positive anomaly values are aligned with the anomalous gravity gradient in the western margin of the Valle Fértil range, coinciding with the Desaguadero–Bermejo lineament (Snyder et al., 1990; Zapata, 1998). Some authors have related this area to a suture zone between Cuyania and Pampia (Alvarez et al., 2012; Chernicoff et al., 2009; Gilbert et al., 2006; Giménez et al., 2000; Introcaso et al., 2004) or between Cuyania and the Famatinian magmatic arc (Cristofolini et al., 2014).

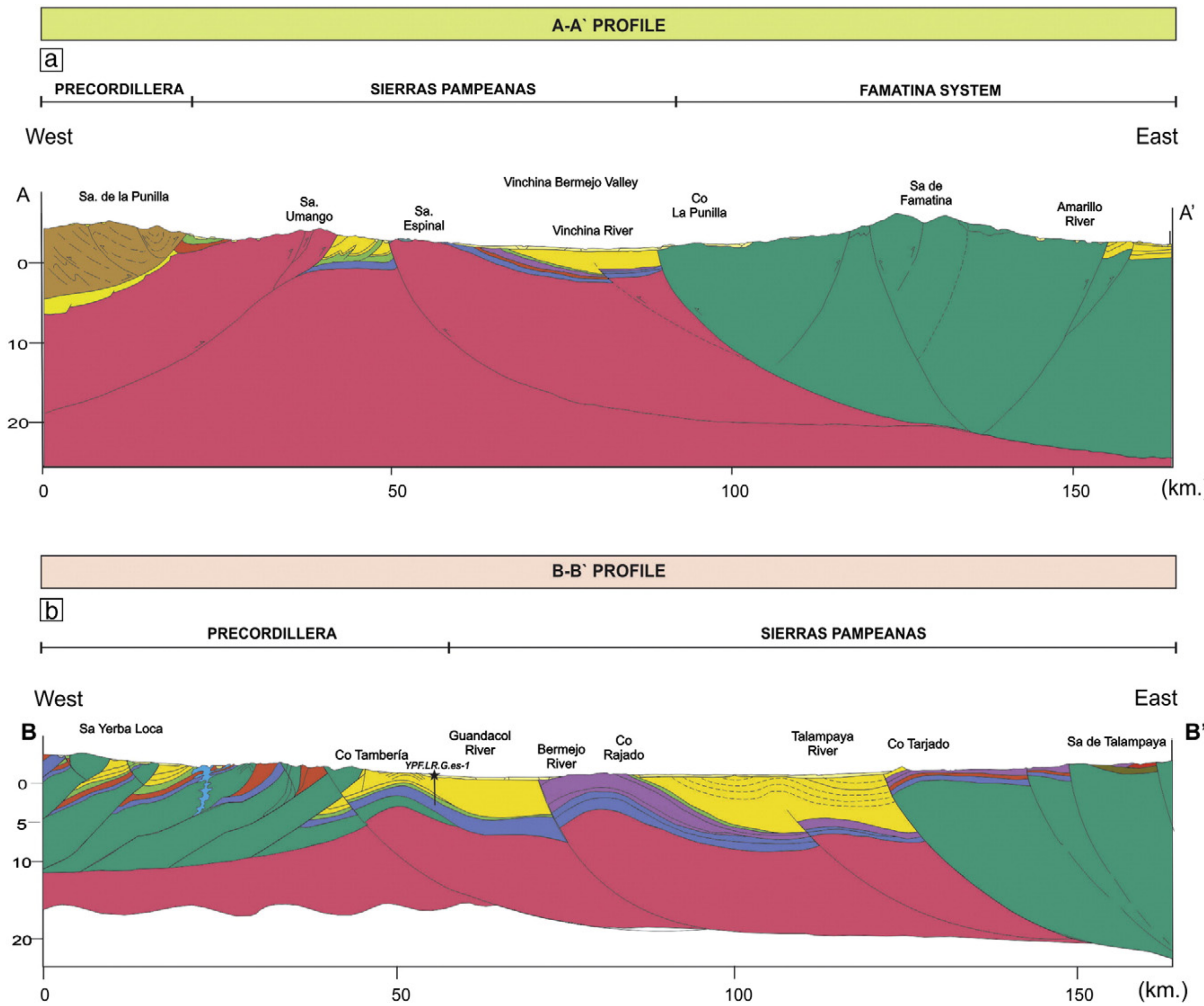

Fig. 3. Balanced geological models in the E–W direction, with 170 km of length (Fauqué et al., 2005). The models show the different geological units intervening in the region of Precordillera, Sierras Pampeanas and Famatina System. a — section A–A′ through the eastern Precordillera–Vinchina Valley and Famatina System, at 29°30′S. b — section B–B′ through the eastern Precordillera, Guandacol basin at the latitudes of the Valle Fértil range (Cerro Rajado), 29°45′S. The references are shown in Fig. 2.

It is well known that the increase of the metamorphic grade increases rock density. This can be quantified on the basis of petrophysical data, for example in Finland meta-mudstones show an increase in density from 2.71 g/cm^3 for rocks of a lower degree up to 2.78 g/cm^3 for garnets in a high metamorphic grade (Elo, 1997; Puranen et al., 1978; Zaffarana et al., 2011). Mogessie et al. (2000) reported density values of 2.95 g/cm^3, 3.02 g/cm^3 and up to 3.05 g/cm^3 for Las Águilas, Viroco and El Fierro intrusives respectively in the San Luis range. These values contrast very well with the gneiss and phyllites with values of 2.71 g/cm^3 reported by Kostadinoff et al. (1998). Zaffarana et al. (2011), measured average values of 2.66 g/cm^3 for the phyllites of the San Luis formation, for the gneiss and schists of the Pringles Complex 2.85 g/cm^3 and 3.10 g/cm^3 for the mafic and ultra-mafic rocks of the Las Águilas Group.

5. Satellite gravimetry and vertical gravity gradient

5.1. Methodology

The vertical gravity gradient (Tzz) highlights mass heterogeneities when the density contrast is significant, especially in the upper crust. However, the gravity anomaly is more effective when the density contrast is relatively low and the geologic structures highlighted are deep; in this case, the Tzz loses resolution. Even though the latter and the gravity anomaly reflect density variations in the crust, they delineate very different sub-superficial characteristics. When both quantities are calculated for terrestrial masses, equivalent geological characteristics are highlighted in a distinct and complementary way (Álvarez et al., 2012; Braitenberg et al., 2011a,b).

To calculate the Tzz, two models were used (EGM2008 from Pavlis et al., 2008 and GOCE-GO_CONS_GCF_2_TIM_R4 from Pail et al., 2011) in a geocentric coordinate system (Fig. 5a and b). The calculation was carried out at 7000 m to ensure that all points were over the topography. The values were calculated on a regular grid of 0.05° cell size, with the maximum degree and order of the harmonic expansion for each model ($N = 2159$ for EGM2008 and $N = 250$ for GOCE). The calculation with EGM2008 presents the advantage of higher spatial resolution, while GOCE gives higher accuracy and homogeneous precision (for more detail see Braitenberg et al., 2011a,b; Alvarez et al., 2012, Álvarez et al., 2013).

A topographic effect correction was applied to eliminate the correlation with topography in both models (Álvarez et al., 2013). The mass elements obtained based on a global relief model (ETOPO1, Amante and Eakins, 2008), were approximated with spherical prisms (Anderson, 1976; Heck and Seitz, 2007; Grombein et al., 2012; among others) of constant density in a spherical coordinate system to take into account

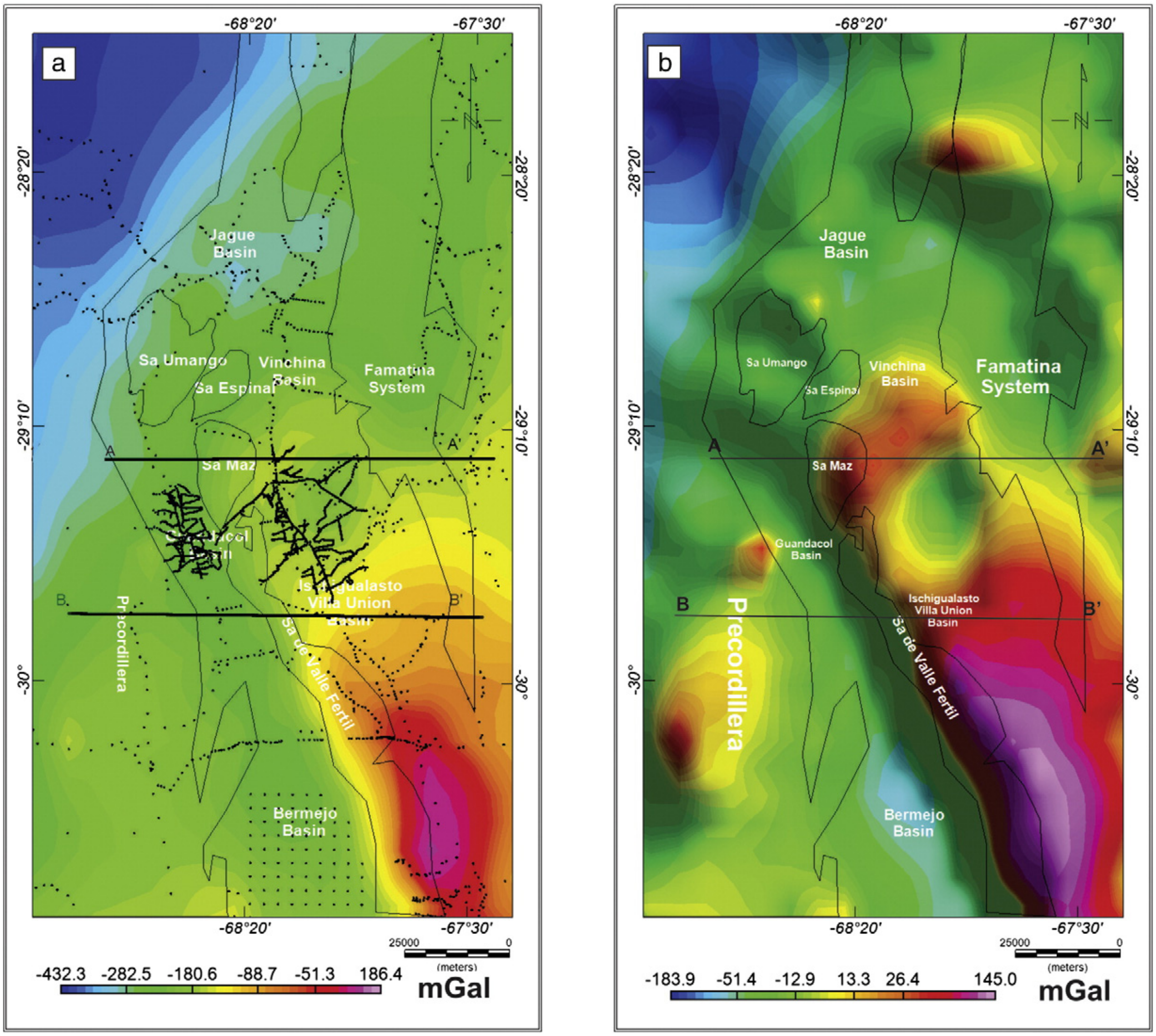

Fig. 4. a — Bouguer anomaly map, with the gravity stations. b — residual Bouguer anomaly map, only the short wave lengths are observed, i.e., considering the gravimetrical effects of the geological structures that are emplaced in the upper and middle crust. Both maps depict the main structures in the area and sections under study, Profiles A–A′ and B–B′.

the Earth curvature (Uieda et al., 2010). A standard density of 2.67 g/cm^3 was used for the masses above sea level.

5.2. Results

By comparing terrestrial Bouguer anomaly maps with vertical gravity gradient (Tzz) from the EGM2008 model, we found good correlation (Fig. 5b). When compared with that obtained from satellite GOCE data (Fig. 5a); they also agree but at higher wavelengths. The Tzz obtained from the EGM2008 model shows a high-resolution anomaly distribution, while the Tzz obtained with GOCE shows a smoother pattern, i.e., a higher wavelength. It can be seen that the GOCE signal shows a regional characteristic in the definition of structures relative to the EGM2008 model.

In both maps, the Bermejo basin is delineated by a low Tzz (up to −20 Eötvös GOCE; −30 Eötvös EGM2008). East of the basin, the high Tzz of the Valle Fértil range (ranging from −3 to +3 Eötvös for GOCE and from +8 to +150 Eötvös EGM2008) can be observed. The Bermejo–Desaguadero lineament shows this density contrast. West of the Bermejo basin, the positive response of the Precordillera can be seen (from −3 to 0 Eötvös GOCE; from −11 to +150 Eötvös EGM2008). The Tzz obtained from GOCE model shows a high gradient value (+156 Eötvös for EGM2008; +3 Eötvös for GOCE) over the Maz range. To the N–E, the Vinchina basin which is separated from the Valle Fértil range to the southeast, the Tzz reveals a lower gradient value.

6. Aeromagnetometry

6.1. Methodology

Aeromagnetic data were available in a total magnetic field (TMI) grid corrected by the daily variation of blocks 4 and 18 of the Argentinean Geological-Mining Service (SEGEMAR). Block 18 corresponds to Famatina and was measured to a nominal flight height of 120 m, with principal lines going north to south at a spacing of 1000 m and control lines running east to west every 7500 m. Block 4 corresponds to the northern Precordillera area, where the nominal flight height was 140 m, with the main lines going north to south at a spacing of 1000 m, and control lines running east to west every 10,000 m.

The aeromagnetic anomaly was calculated for each block described, removing the IGRF field (International Geomagnetic Reference Field) from each block at the acquisition date (Blakely, 1995). We created a mosaic with both grids following the methodology proposed by Ruiz et al. (2011), for which terrestrial measurements of the Total Magnetic Intensity were used, belonging to IGSV (Fig. 6a).

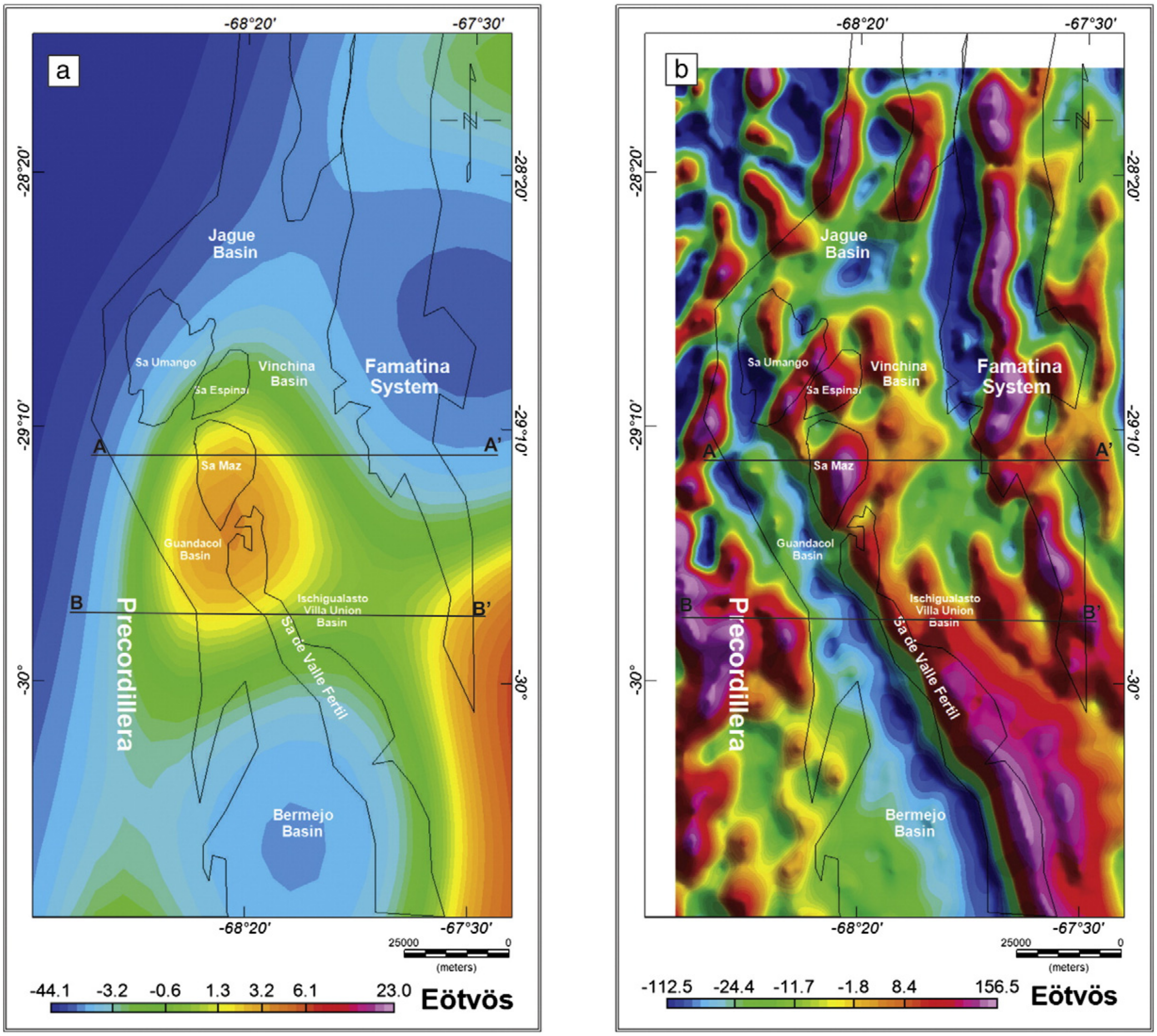

Fig. 5. a — vertical gravity gradient (Tzz) based on satellite GOCE data (up to degree/order: 250), showing the anomaly north of the Valle Fértil range and west of Famatina. b — Vertical gravity gradient based on EGM2008 model (up to degree/order: 2159). In both maps, cross sections are represented by solid black line (A–A′ and B–B′) and the main structures of area are also highlighted.

6.2. Results

The magnetic anomaly map shows two regions well-differentiated in their positive values; they are: the Vinchina basin, the Famatina System, and the Central South of the Precordillera region. The rest of the map observes regions of less positive anomalies in the basement of the negative magnetic anomalies which increase in the Andean Cordillera region.

6.3. Reduction to pole of magnetic data

6.3.1. Methodology

Reduction to pole (RTP) (Baranov, 1957; Phillips, 2007) is a magnetic data processing method that removes the asymmetry caused by the non-vertical direction of magnetization (the anomaly reduced to the pole is located above the causing body). The RTP method takes the total magnetic field observed and transforms it to produce the magnetic map that would have resulted if the study zone were in the terrestrial magnetic pole (magnetic inclination 90°). Assuming that the entire observed magnetic field is due to the induced magnetic effects, the application of this technique facilitates comparison with gravimetric data (Fig. 6b).

6.4. Results

The reduction to the pole of magnetic anomalies displays a range of values from −400 nT to +430 nT. Unfortunately, they do not cover the entire area under study, especially in the southern section. However, an important positive anomaly can be observed in the northern section: this anomaly widely surpasses the Vinchina basin and extends toward the Famatina System. Additionally, negative values can be seen in the west, over the Maz range and north of the Precordillera. In contrast, in the southern section (B–B′), the positive values are located to the west over the Precordillera and a portion of the Guandacol–Bermejo basin (Fig. 6b).

7. Sampling of densities and magnetic susceptibilities

Densities used in the 2D direct models were collected by means of surface samples in some representative sectors, as well as through mineralogical modal rock composition (Pérez Luján et al., in press and references therein) in the occidental Precordillera zone. Authors such as: Giménez et al., 2000; Martínez et al., 2003 and Azeglio et al., 2010, reported similar densities in neighboring gravi-magnetometric basin models.

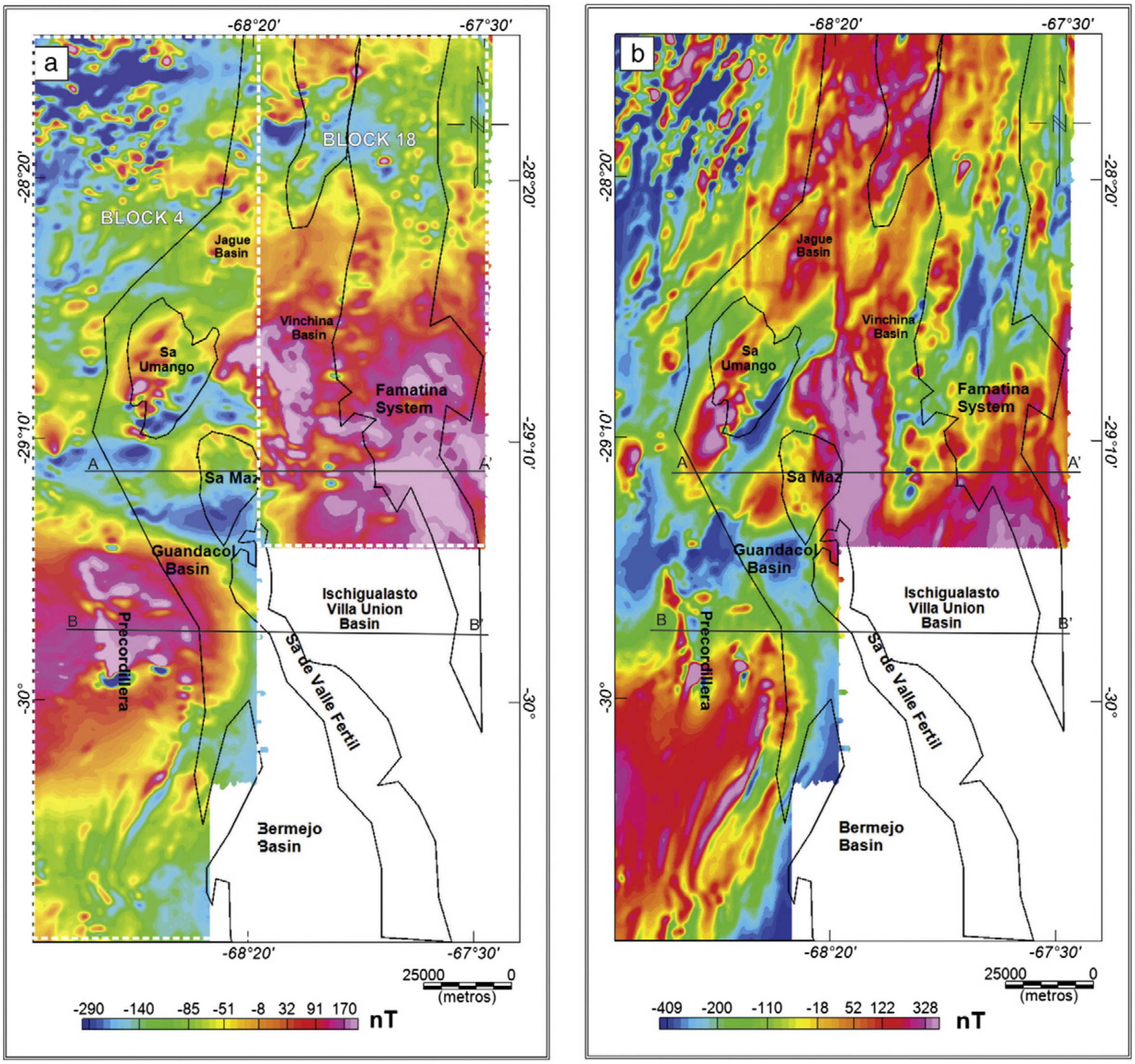

Fig. 6. a — total magnetic anomaly field map: white shaded area shows gridded blocks of aeromagnetic flights. Block 4 corresponds to north of Precordillera and Block 18 to Famatina. In both blocks the IGRF was discounted and corrected by diurnal variations. b — reduced magnetic pole anomaly map where the positive anomaly on the Vinchina basin is clearly observed. In both maps the balanced geological profiles are shown by the continuous black line [A–A′–B–B′] and the principle structures of the study zone. The aeromagnetic flights do not cover the entire study area.

Geologic samples (minimum 10 samples per unit) were collected from the most representative units of the study region. The Rock & Soil Mechanics Laboratory [UNSJ] calculated the average density based on the method of double weighing with paraffin for each sample, with an error of one hundredth [1/100th] of a g/cm^3 (see Table 1). The magnetic susceptibilities were obtained both in situ (in borings) and from manual samples using the susceptibility-meter (Kappameter KT-6 with a precision of 10^7) (see Table 1).

8. 2D gravi-magnetometric direct models

8.1. Methodology

Forward gravity-magnetic models from two balanced geological cross-sections, are indicated in Fig. 7a and b as A–A′ and B–B′. The initial forward gravity-magnetic models were developed using the GMSYS software. We assigned densities and magnetic susceptibilities (Table 1) to the different polygons that represent the geologic units of interest. Different geometric configurations for each polygon were

Table 1
Density and magnetic susceptibility values of rock samples obtained in borings, and outcrops corresponding to the geological units present in the study area.

		Average (ε ± 0.001) densities (g/cm^3)	Average susceptibilities
	Quaternary	2.20	2.05×10^{-5}
	Tertiary	2.39	61.3×10^{-5}
	Cretaceous	–	–
	Triassic	2.07	24.4×10^{-5}
	Permian	–	–
	Carboniferous	2.59	24.72×10^{-5}
	Devonian–Silurian	–	–
	Ordovician	2.66	11.05×10^{-5}
	Camrian–Precamb	2.68	21.85×10^{-5}

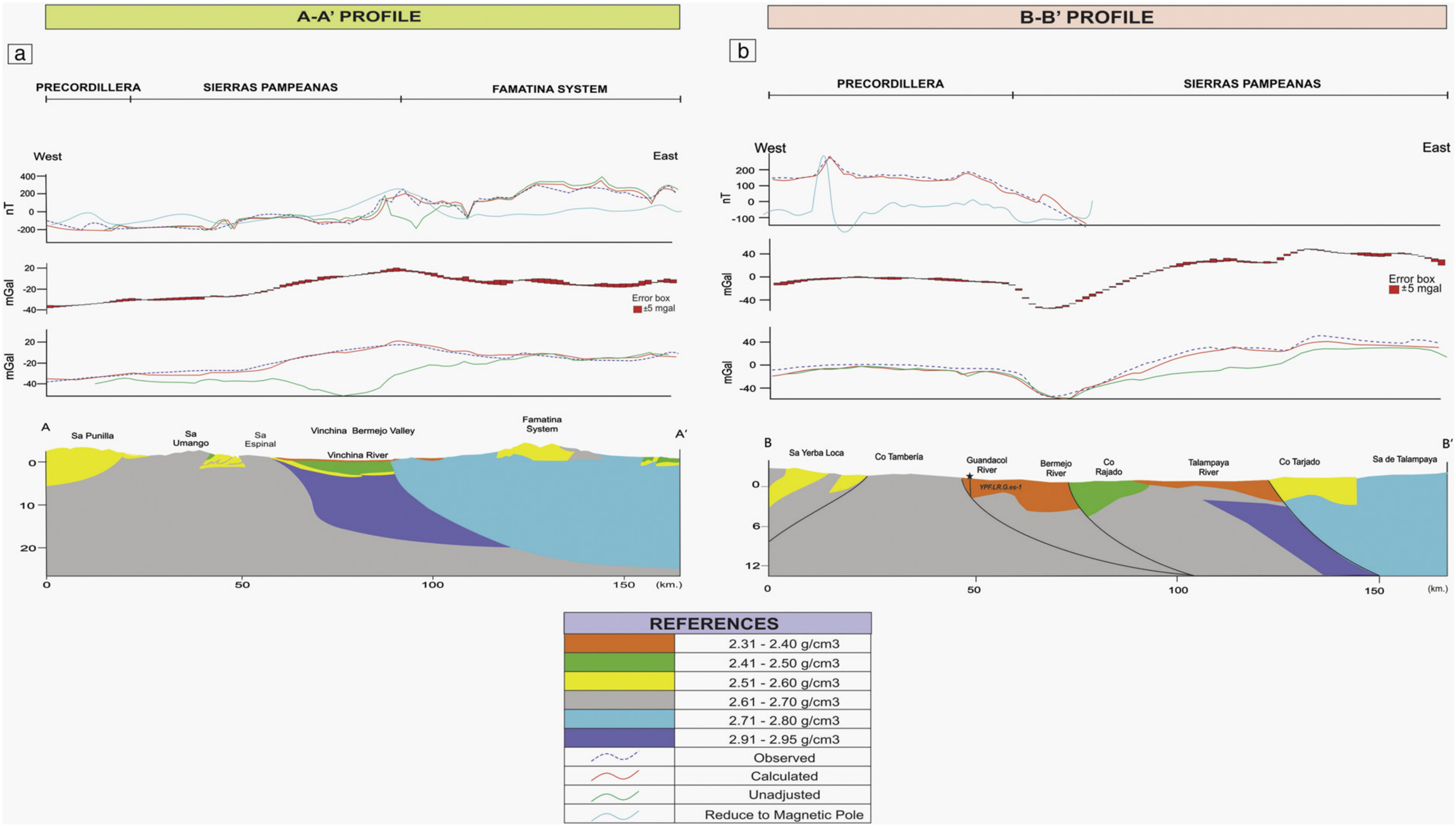

Fig. 7. 2D geophysical models, A–A′ and B–B′, both sections were modeled with gravity and magnetism data. Density ranges are indicated in g/cm^3, three curves can be observed in each one of the profiles: the blue-dotted line correspond to observed curves of the measured data, red lines are calculated from the densities and magnetic susceptibilities, green curve makes reference to an unadjusted model without considering the dense masses located below the Vinchina basin, East of Cerro Rajado and the light blue curve determine that reduced to pole of the magnetic anomaly.

tested, in order to fit the model response to the observed data; the final model is that of best fitting (Fig. 7a and b).

The region under study presents a great lithological variability; for this reason we used different density values for each of the polygons, ranging from 2.31 g/cm^3 to 2.40 g/cm^3 for the basins. These values are typical of sedimentary filling found in neighboring basins (Giménez et al., 2000; Ruiz and Introcaso, 2000; Introcaso et al., 2004; Azeglio et al., 2010; among others). To model the metamorphic basement of the Sierras Pampeanas, we used a range of densities from 2.61 g/cm^3 to 2.70 g/cm^3. Similar densities to widely-used values reported by many authors for crustal models, e.g., the Valle Fértil range (Giménez et al., 2000; Zaffarana et al., 2011), the Famatina System (Martínez et al., 2003) and the San Luis range (Kostadinoff et al., 2010). In the Precordillera, we used a density range from 2.51 g/cm^3 to 2.6 g/cm^3, typical of sediments (Giménez et al., 2000; Kostadinoff et al., 2004; Martínez et al., 2003; Ruiz and Introcaso, 2000).

Were modeled anomalous high-density bodies using a density variation between 2.91 g/cm^3 to 2.95 g/cm^3; as done in previous works in the area under study, mainly in the Bermejo basin (Giménez et al., 2000; Kostadinoff et al., 2004; Martínez et al., 2003; Ruiz and Introcaso, 2000). Pérez Luján et al. (in press) worked in the Precordillera occidental zone, south of the study zone, and reported density values in ultra-mafic rocks of approx. 2.88 g/cm^3 to 3.28 g/cm^3, obtained from modal mineralogical rock composition.

The magnetic susceptibility values (Table 1) obtained (from hand samples and outcrops) for the crystalline basement of the Sierras Pampeanas are significantly lower than the values reported for ophiolitic bodies found in the region (Chernicoff et al., 2009; Kostadinoff et al., 2010).

The geometry of the crust–mantle interface (Moho) presents maximum values along the Andean axis (66 km) and about 35 km on the study area (Weidmann et al. (2013)). The Cordillera de Los Andes is associated with a pronounced crustal "root", whereas beneath the range of Famatina System and Sierras Pampeanas, the crustal thickness decreases significantly. These results are consistent with Introcaso et al. (2000) and Giménez et al. (2000).

8.2. Results

In the 2D geological–geophysical models (Fig. 7), it was necessary to introduce high densities (≈3.0 g/cm^3), in both Profiles A–A′ and B–B′, below the Vinchina basin, west of the Famatina System and east of the Cerro Rajado in the Valle Fértil range, respectively. In this way, were achieved a good fitting between the Bouguer residual anomaly and magnetic anomaly curves (observed data—blue dot curves) and the response obtained for both models. This indicates a lack of correspondence between the existing geological information and the signals from potential field data. The need of considering higher densities in the model obtained from potential field data; probably indicates a misinterpretation of the preceding geological models.

In order to demonstrate the lack of adjustment between both curves, observed and calculated (blue-dotted line & red curve respectively), both profiles were modeled without placing dense bodies below the Vinchina basin and Cerro Rajado respectively, obtaining the green curve (Fig. 7) where the lack of adjustment is notorious. This shows the need of incorporating materials of ≅ 3.0 g/cm^3 in order to achieve a better adjustment between both (observed and calculated) curves. It also demonstrates that adjustment cannot be obtained by only changing the geometry of the polygons (potential forward modeling ambiguity). This is evident in both sections modeled with gravity and magnetism (A–A′–B–B′).

Statistical analyses were made of the absolute residual between the observed data and the model response along both profiles. Statistical parameters for the difference between observed and calculated data for both profiles are shown on Table 2. In Fig. 7 are represented the error (red box) for the profiles A–A′ and B–B′ respectively. For profile A–A′ we obtained a maximum difference of 17.257 mGal, while for profile B–B′ we obtained a maximum difference of 9.171 mGal, which corresponds to approximately the 10% of the peak-to-peak values of the signal (see Table 2).

Table 2
Statistical parameters for the 2D models: gravity observed and calculated from the inverse modeling of the balanced sections (A–A′–B–B′). This shows minimum/maximum values for each plotted curve in Figs. 8 and 9, the maximum difference, the average, and standard deviation in both curves represented.

Profile	A–A′	B–B′
Min. value observed	−40.551	−51.289
Max. value observed	26.348	50.584
Min. value calculated	−40.357	−48.017
Max. value calculated	30.553	53.889
Statistical parameters for the absolute difference		
Max. value of difference	17.256	9.171
Average difference	3.557	2.196
Standard deviation	3	1.664

Statistical parameters for the absolute difference are: average difference = 3.556 mGal, standard deviation = 2.919 mGal, maximal value of difference = 17.256 mGal for profile A–A′ and average difference = 2.196 mGal, standard deviation = 1.664 mGal, and maximal value of difference = 9.171 mGal for profile B–B′. The maximum mismatch between the observed data and the gravimetric response models is due to the vagueness in balanced models. This is due to use of what probabilistic models are generated, based on balanced surface geologic data. It is impossible to achieve a perfect adjustment in both curves (observed & calculated). Since Vinchina basin has a thickness varying between 7 and 10 km and there are no outcrops to justify the high densities found below this basin, it is impossible to determine the geometry of these masses by means of the methods used. Therefore this is a model requiring multiple interpretations.

9. Inverse modeling

9.1. Methodology

For inverse gravity modeling they used the 'VOXI' technique (Geosoft), for residual Bouguer data surveys. It performed calculation of the inversion model by defining an area greater than the study region (Fig. 8). Subsequently the number of cells (voxels) was defined: 285 × 315 voxels, and the minimum error = 1 mGal. The model consists of 3 layers: topography, plane of mean sea level, and basement. The reference density for calculation was 2.67 g/cm^3. The layers of topography and mean sea level remain fixed, while the basement layer was variable.

Ellis et al. (2012) developed the Magnetic Vector Inversion (MVI) method to directly model the vector of magnetization based only on anomalous TMI data. The method gives the modelling optimization process the freedom to orient the direction of magnetization to best fit the observed data. Notably, the MVI method does not concern itself with the reason for varying magnetization direction, which is left to the interpreter to ponder together with other information that may be at hand.

9.2. Results

Fig. 8 presents the results of the gravimetric inversion section using the VOXI technique, from the Bouguer residual anomaly and the topography. We obtained a density model up to a depth of 13 km. The disposition of the X and Y axes of the structures is displayed in high density contrasts. The presence of high density materials is also evident with this technique (VOXI). In section (A–A′) these materials are approximately ≅ 3.0 g/cm^3 keeping in mind that the normal values in Vinchina basin should be approximately 2.31 a 2.40 g/cm^3 (Fig. 8a). To the South,

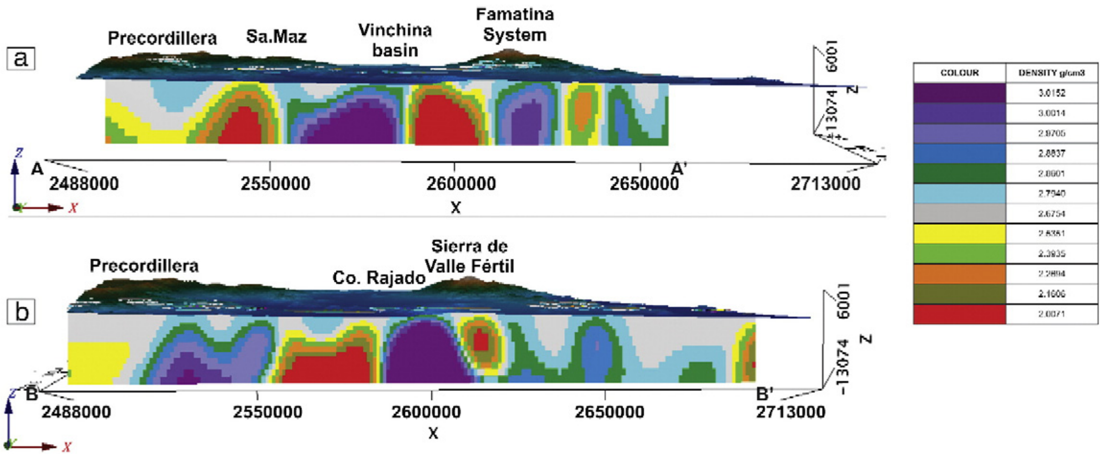

Fig. 8. Sections A–A′ and B–B′ are found located at the same latitude where 2D gravi-magnetometric modeling was carried out (Fig. 7). These sections were made through use of the Voxel technique. The cool color [blue & purple] represent high-density values of approx. ≈3.0 g/cm^3. Whereas the warm colors (red, orange, yellow) represent low densities, shown in each profile. a — north section A–A′ which cuts across the Precordillera, Sierra de Maz, Vinchina basin to the Famatina System. The high densities are observed below the Vinchina basin. b — south section B–B′ which crosses the Precordillera, Cerro Rajado (Valle Fértil range) to the Sierras Pampeanas. The high densities are concentrated to the East of Cerro Rajado.

in Section B–B′, these materials are located to the East of Cerro Rajado (Valle Fértil range).

The magnetic susceptibility model is presented in Fig. 9. This model was realized through the modern MVI technique (Magnetization Vector Inversion), using Geosoft VOXI platform. Results obtained from the magnetic data inversion of the corresponding polygon were derived from the basis of the DEM that is observed in Fig. 9a. The result of the magnetic inversion is shown in Fig. 9b, where the model reached a maximum depth of 13.9 km and the values of maximum susceptibility are located below the Vinchina basin and Cerro Rajado. In part C of the same figure, the observable values corresponding to the western sector have been filtered (over the X axis), in order to observe the susceptibility distribution of the region under study for this work, in greater detail.

10. Discussion

In the South Central Andes region, a gravimetric and magnetic-based study was performed. We used geological information and physical properties of the rocks, modeling two W–E geological sections that cross the Vinchina basin in the northern section and the Guandacol basin in the southern one.

There could be different interpretations for these models (cross-sections in Fig. 7). Our results represent a new proposal based on the background and new data that involve collisions between the Cuyania terrain with the Gondwana continent and the Famatinian magmatic arc. The calculated gravimetric and magnetic responses were compared with the observed gravimetric and magnetic data, which resulted in a significant misfit between the two curves (observed and calculated).

The maximum difference is produced in profile A–A′, centered at the Vinchina basin. In profile B–B′ the maximum difference is located in the region to the east of Cerro Rajado, in the Valle Fértil range. The difference between observed and calculated anomalies in profiles A–A′ and profile B–B′ would indicate the presence of denser bodies in these sectors. Toward the North of the Vinchina basin the anomaly presents an intermediate wavelength. Although this finding can be associated with small structures within the upper crust it can also be produced by intermediate size structures located at deeper levels. The latter would be consistent with the typical collision zone environment with accretionary structures such as the relics of accretion wedges identified in Cuyania and Pampia in the Valle Fértil range or of Cuyania in the Famatinian magmatic arc. This collision generated ophiolites, high-grade metamorphism and volcanism.

The observed misfit can be only corrected with denser materials than mean value 2.67 g/cm^3 located at the base of Vinchina basin and east of Cerro Rajado, since no surface evidence exists for this type of rock in section A–A′. This result was consistent with the inversion of the gravity and magnetic anomalies that constrained the location of the higher density masses (in the case of gravity) and major susceptibilities (the case of magnetism).

The satellite information concerning the vertical gravity gradient, Tzz (GOCE and EGM2008), are coherent with the terrain measurement. Although the feature of lower resolution, positive anomaly values can be observed in the study area; supporting the hypothesis of the existence of a dense mass located below these geological structures.

The development of this research has followed the deductive hypothetical methodology. Which begins with observed data (Bouguer & Magnetic anomaly) conveniently attempted through 'separation of effect' techniques. We interpreted that below Vinchina basin and Cerro Rajado, there could be bodies of major density. These bodies would indicate positive residual gravimetric responses and at medium- wavelengths. This is mainly observed in the Vinchina basin zone of thick sedimentation.

The majority of the existent information is from surface from which Fauqué et al. (2005) performed two balanced geological sections, over which we made two gravimetric models. To do this, densities were assigned to each one of the geological formations identified on the terrain. The objective was to calculate the sum of gravity effects corresponding to each geological structure and compare it to the Bouguer anomaly. The adjustment between the anomalies observed and calculated was obtained by incorporating balanced bodies of maximum density (≅3 g/cm^3) in each geological section, corroborating the original hypothesis. If there is only one possibility for adjustment, then it may not be unusual to encounter positive gravity anomaly below thick basin sediments, considering that the geometry of the Moho is almost flat (Gimenez et al., 2009, 2000; Introcaso et al., 2000).

To verify this result we performed inversion models based on gravimetric and magnetic data, applying well-known (commercial), modern techniques. These models separate from the residual Bouguer anomaly and magnetic anomalies respectively. They focus on the contour conditions and built a box of models of with topography and anomalies. In the case of gravity, a standard density calculation of 2.67 g/cm^3 was assigned. As a result, a cube of information with density variations or magnetic susceptibility accordingly was obtained.

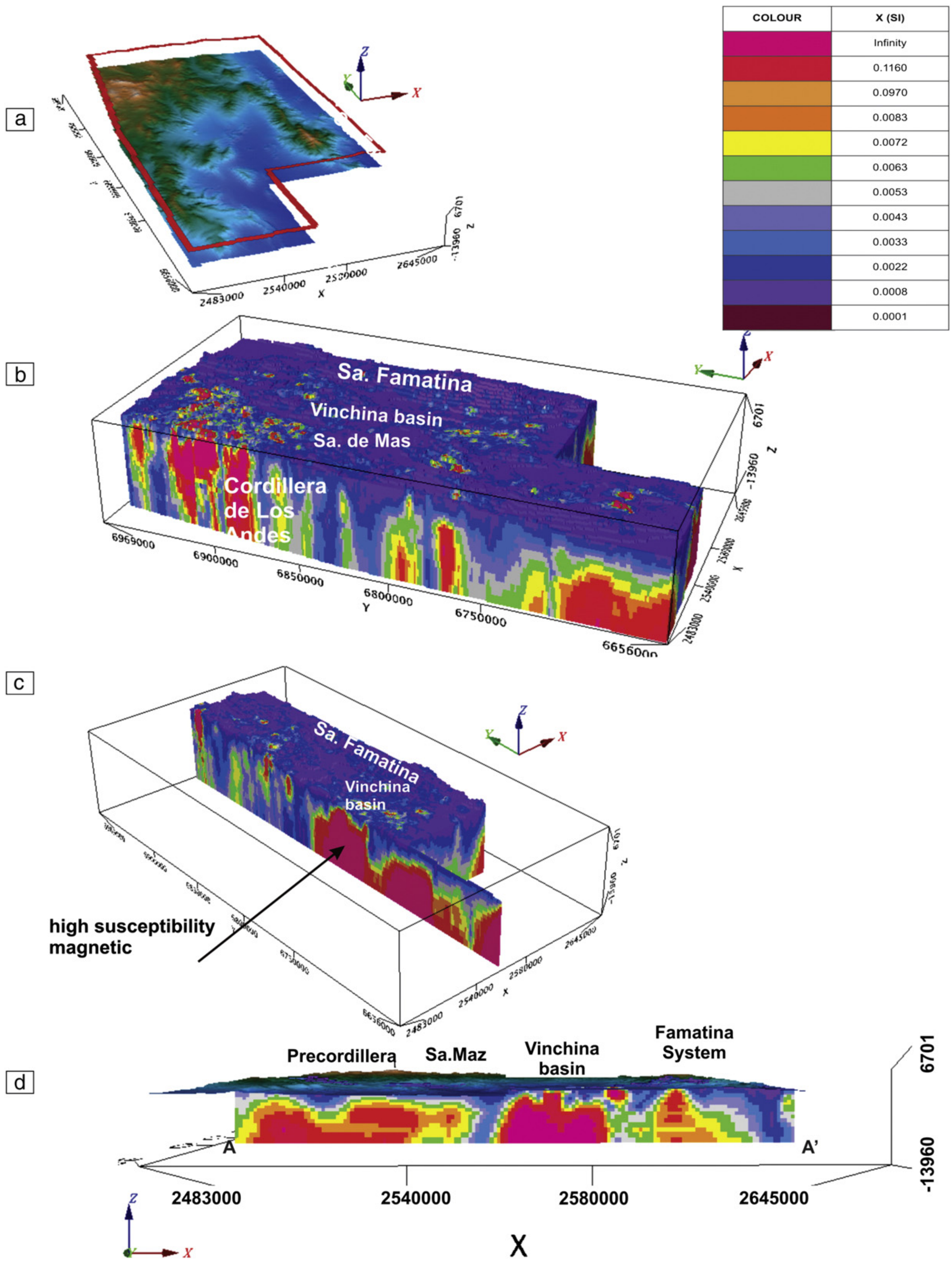

Fig. 9. Inversion model of magnetic anomaly, using the Voxel technique. a — area in which the magnetic inversion is applied represented by a DEM. b — model of inversion in which red colors indicate high magnetic susceptibility and blue colors low susceptibility. c — the information in coordinate x has been filtered, in order to observe the higher susceptibilities below the Vinchina basin and west of Cerro Rajado. d — section A–A′ where the high susceptibilities are shown below the Vinchina basin. The aeromagnetic data does not cover the entire study area, thus it was impossible to do profile B–B′.

Using this technique, we could verify the existence of denser bodies with high-magnetic susceptibility in some regions previously pointed out by other authors, reinforcing the original hypothesis.

The new geophysical and geological results discussed here agree with the proposal of Otamendi et al. (2009, 2012), and Cristofolini et al. (2010, 2014). They suggested that Valle Fértil range is made up of igneous rocks integrating the Famatina magmatic arc, whose structural evolution shows the effects of a post-magmatic tectonic event. This event is linked to the exhumation of the deepest part of the arc. Moreover it appears to be the result of the collision between the Cuyania terrane and the western Gondwana margin. Finally, the collision of the micro-continents composing Cuyania that generated the interruption of the magmatic activity between 479 and 465 million years ago, were followed by the shortening, piling and exhumation processes throughout the Famatinian surface crust.

11. Conclusions

This research was developed in the foreland environment of the Vinchina basin and north of the Valle Fértil range, beginning with a treatment of gravimetric–magnetic data supported by geological information. We encountered anomalous gravity and magnetic values which we linked to the high-density/susceptibility bodies located in the upper crust.

The collision of Cuyania with the Western margin of Gondwana was generated during an important oogenesis [Famatiniana] of Ordovician age. This affected both Gondwana as well as Cuyania micro-continent, giving rise to different units of mafic and ultra-mafic rocks, represented by ophiolitic sequences. These rocks were identified by diverse authors throughout the Precordillera border.

The results obtained here allowed us to conclude that these anomalous bodies (high-density rocks) found, could be relics of the accretion wedge between Cuyania and the Famatina magmatic arc.

Acknowledgments

We would like to express our thanks to the Grosso Group Company and the Argentinean Geological Mining Service (SEGEMAR) for their aero-magnetic flights. This study has been partially financed by projects PICT 2010-2401 (National Agency for Scientific and Technological Promotion) and CONICET. We also recognize and appreciate the invaluable comments of Dr. Victor Ramos that helped enormously in the clarity of the manuscript.

References

Aceñolaza, F.G., Toselli, A.J., Bernasconi, A., 1971. La Precordillera de Jagüé, La Rioja, Argentina. Su importancia geológica y estructural. Acta Geol. Lilloana 11 (14), 257–290 (San Miguel de Tucumán).

Aceñolaza, F.G., Toselli, A.J., 1976. Consideraciones estratigráficas y tectónicas sobre el Paleozoico inferior del Noroeste Argentino. 2 Congreso Latinoamericano de Geología 2 pp. 755–764 (Caracas).

Aceñolaza, F.G., Toselli, A.J., 1988. El Sistema de Famatina, Argentina: su interpretación como orógeno de margen continental activo. 5° Congreso Geológico Chileno, Actas 1, pp. A55–A67 (Antofagasta).

Aceñolaza, F.G., Miller, H., Toselli, A.J., 2002. Proterozoic–Early Paleozoic evolution in western South America — a discussion. Tectonophysics 354, 121–137.

Allmendinger, R., Jordan, T.E., Palma, M., Ramos, V.A., 1982. Perfil Estructural de la Puna Catamarqueña (25°–27°S), Argentina. 5° Congreso Latinoamericano de Geología, Actas 1, pp. 499–518.

Alvarez, O., Gimenez, M.E., Braitenberg, C., Folguera, A., 2012. GOCE satellite derived gravity and gravity gradient corrected for topographic effect in the South Central Andes region. Geophys. J. Int. 190 (2), 941–959. http://dx.doi.org/10.1111/j.1365-246X.2012.05556.x.

Álvarez, O., Giménez, M., Braitenberg, C., 2013. Nueva metodología para el cálculo del efecto topográfico para la corrección de datos satelitales. Revista de la Asociación Geológica Argentina (En prensa, Junio 2013).

Amante, C., Eakins, B.W., 2008. ETOPO1 1 Arc-Minute Global Relief Model: Procedures, Data Sources and Analysis. 1st ed. NOAA, National Geophysical Data Center, Boulder, Colorado, USA, p. 54.

Anderson, E.G., 1976. The effect of topography on solutions of Stokes' problem. Unisurv S-14, Rep, School of Surveying, University of New South Wales, Sydney (252 pp.).

Astini, R.A., Dávila, F.M., 2002. El Grupo Cerro Morado (Ordovícico Medio) en el Famatina (28°–29°S), Andes Centrales del oeste argentino. Rev. Geol. Chile vol. 29, 241–254.

Astini, R.A., Martina, F., Dávila, F.M., 2011. La Formación Los Llantenes en la Precordillera de Jagüé (La Rioja) y la identificación de un episodio de extensión en la evolución temprana de las cuencas del Paleozoico superior en el oeste argentino. Andean Geol. 38 (2), 245–267.

Azeglio, E.A., Giménez, M.E., Introcaso, A., 2010. Análisis estructural de la cuenca de Las Salinas y su relación con la acumulación de sedimentos eólicos en el área Médanos Negros. Rev. Asoc. Geol. Argent. 67 (2) (Buenos Aires).

Baldis, B., Peralta, S.H., Villegas, R., 1989. Esquematizaciones de una posible transcurrencia del terrane de Precordillera como fragmento continental procedente de áreas pampeano-bonaerenses. Correlación Geol. 5 (8), 1–100.

Baranov, V., 1957. A new method for interpretation of aeromagnetic maps: pseudo-gravimetric anomalies. Geophysics 22, 359383.

Barazangi, M., Isacks, B., 1976. Spatial distribution of earthquakes and subduction of the Nazca plate beneath South America. Geology 4, 686–692.

Blakely, R., 1995. Potential Theory in Gravity and Magnetic Applications. University Press, Cambridge (441 pp.).

Bodenbender, G., 1922. El Nevado de Famatina. Provincia de La Rioja Anales de la Dirección Nacional de Minas y Geología XVI (1). Buenos Aires.

Braitenberg, C., Mariani, P., Pivetta, T., 2011a. GOCE observations in exploration geophysics. Proceedings of '4th International GOCE User Workshop', Munich, Germany, 31 March–1 April 2011 (ESA SP-696).

Braitenberg, C., Mariani, P., Ebbing, J., Sprlak, M., 2011b. The enigmatic Chad lineament revisited with global gravity and gravity-gradient fields. In: Van Hinsbergen, D.J.J., Buiter, S.J.H., Torsvik, T.H., Gaina, C., Webb, S.J. (Eds.), The Formation and Evolution of Africa: A Synopsis of 3.8 Ga of Earth History. Geol. Soc. Lond., Spec. Publ. 357, pp. 329–341. http://dx.doi.org/10.1144/SP357.18.

Briggs, I.C., 1974. Machine contouring using minimum curvature. Geophysics 39, 39–48.

Caminos, R., 1972. Perfil geológico de la Cordillera entre los 28°00 y los 28°30′ de latitud sur, provincia de La Rioja, República Argentina. Rev. Asoc. Geol. Argent. 27 (1), 71–83 (Buenos Aires).

Caminos, R., 1979. Descripción Geológica de las Hojas 21f y g Sierras de Las Minas y Ulapes, provincias de La Rioja y San Luis, Servicio Geológico Nacional. Bolet 172 (Buenos Aires. (Inédito)).

Caminos, R., Fauqué, L., Cingolani, C., Varela, R., Morel, E., 1993. Estratigrafía y estructura del evónico-Carbonífero en el sector septentrional de la Sierra de la Punilla, Precordillera de La Rioja y San Juan. 12° Congreso Geológico Argentino y 2° Congreso de Exploración de Hidrocarburos, Actas 2, pp. 31–41 (Mendoza).

Chernicoff, C.J., Zappettini, E.O., Santos, J.O.S., 2009. Evidencias del orógeno pampeano en la provincia de La Pampa, Argentina. 14° Reunión de Tectónica. Libro de Resúmenes 62 (Río Cuarto).

Chernicoff, C.J., Zappettinii, E.O., Santos, J. O.S., Allchurch, S.Y., Mcnaughton, N.J., 2010. The southern segment of the Famatinian magmatic arc, La Pampa province, Argentina. Año 17. Gondwana Research, Lugar: Amsterdam, pp. 662–675.

Collo, G., Dávila, F.M., Nóbile, J., Astini, R.A., Gehrels, G., 2011. Clay mineralogy and thermal history of the Neogene Vinchina Basin, Central Andes of Argentina: analysis of factors controlling the heating conditions. Tectonics 30 (4) (art. no.).

Cristofolini, E.A., Otamendi, J.E., Tibaldi, A.M., Martino, R.D., Baliani, I., 2010. Geología de la porción occidental de la sierra de Valle Fértil, San Juan, a partir de observaciones en la quebrada de Otarola. Rev. Asoc. Geol. Argent. 67 (521e), 535.

Cristofolini, E.A., Otamendi, J.E., Walker Jr., B.A., Tibaldi, A.M., Armas, P., Bergantz, G.W., Martino, R.D., 2014. A Middle Paleozoic shear zone in the Sierra de Valle Fértil, Argentina: records of a continent–arc collision in the Famatinian margin of Gondwana. J. S. Am. Earth Sci. 56, 170e185.

Dalla Salda, L., Cingolani, C., Varela, R., 1992. Early Paleozoic orogenic belt of the Andes in southwestern South America. Results of Laurentian–Gondwana collision? Geology 20, 617–620.

Dahlquist, J.A., Rapela, C.W., Baldo, E., 2005a. Petrogenesis of cordierite-bearing S-type granitoids in Sierra de Chepes, Famatinian orogen, Argentina. J. S. Am. Earth Sci. 20, 231–251.

Dahlquist, J.A., Rapela, C.W., Pankhurst, R.J., Baldo, E., Saavedra, J., Alasino, P.H., 2005b. Los granitoides de la sierra de Chepes y su comparación con granitoides paleozoicos de las Sierras Pampeanas: implicancias para el orógeno famatiniano. Geología de la provincia de La Rioja — Precámbrico–Paleozoico Inferior. In: Dahlquist, J.A., Baldo, E.G., Alasino, P.H. (Eds.), Asoc. Geol. Argent. D Publ. Espec. 8, pp. 87–108 (In Spanish).

Dahlquist, J.A., Pankhurst, R.J., Rapela, C.W., Casquet, C., Fanning, C.M., Alasino, P., Baez, M., 2006. The San Blas Pluton: an example of Carboniferous plutonism in the Sierras Pampeanas, Argentina. J. S. Am. Earth Sci. 20, 341–350.

Dalziel, I.W.D., Dalla Salda, L.H., Gahagan, L.M., 1994. Paleozoic Laurentia–Gondwana interaction and the origin of the Apalachian–Andean mountain system. Geol. Soc. Am. Bull. 106, 243–252.

Dávila, F.M., Astini, R.A., 2003a. Discordancias progresivas en los depósitos pre-neógenos del Famatina (Formación del Crestón), La Rioja, Argentina y su implicancia en la cronología evolutiva del antepaís andino. Rev. Asoc. Geol. Argent. 58, 109–116.

Dávila, F.M., Astini, R.A., 2003b. Early Miocene synorogenic strata in Famatina (Central Andean broken foreland): wedge-top depozone, proximal foredeep sedimentation or a different setting? Latin American Congress of Sedimentology. 3, pp. 182–183 (Belém, Brazil)

De Alba, E., 1954. Descripción geológica de la hoja 16C Villa Unión (provincia de La Rioja). Dirección Nacional de Minería. Boletín n°82.

De Alba, E., 1979. Descripción de la Hoja Geológica 16d, Chilecito, Provincia de La Rioja. Servicio Geológico Nacional. Boletín 163.

Ellis, R.G., de Wet, B., MacLeod, I.N., 2012. Inversion of magnetic data for remanent and induced sources. 22nd International Geophysical Conference and Exhibition ASEG, Expanded Abstracts, pp. 1–4.

Elo, S., 1997. Interpretations of the gravity anomaly map of Finland. Geophysic 33 (1), 51e80.

Fauqué, L.E., Villar, L.M., 2003. Reinterpretación estratigráfica y petrológica de la Formación Chuscho, Precordillera de La Rioja. Rev. Asoc. Geol. Argent. 58, 218–232.

Fauqué, L.E., Limarino, C., Vujovich, G., Dávila, L.F., Cegarra, M., Escosteguy, L., 2005. Carta Geológica de Villa Unión 2969-IV, 2005. SEGEMAR.

Finney, S., Gleason, J., Gehrels, G., Peralta, S., Aceñolaza, G.F., 2003. Early Gondwana connection for the Argentine Precordillera terrane. Earth Planet. Sci. Lett. 205, 349–359.
Finney, S.C., 2007. The para-authochtonous Gondwanan origin of the Cuyania (Greatther Precordillera) terrane of Argentina. A re-evaluation of evidence used for support an allochthonous Laurentian origin. Geol. Acta 5 (2), 127–158.
Fisher, N.D., Jordan, T., Brown, L., 2002. The structural and stratigraphic evolution of La Rioja Basin, Argentina. J. S. Am. Earth Sci. 15, 141–156.
Furque, G., 1972. Precordillera de La Rioja, San Juan y Mendoza. In: LEANZA, A.F. (Ed.)- Geología Regional Argentina, Academia Nacional de Ciencias, pp. 237–282 (Córdoba).
Gilbert, H., Beck, S., Zandt, G., 2006. Lithospheric and upper mantle structure of Central Chile and Argentina. Geophys. J. Int. 165, 383–398.
Giménez, M., Martínez, M.P., Introcaso, A., 2000. A crustal model based mainly on gravity data in the area between the Bermejo Basin and the Sierras de Valle Fértil—Argentina. J. S. Am. Earth Sci. 13 (3), 275–286 (Agosto 2000).
Gimenez, M.E., Martinez, M.P., Jordan, T., Ruíz, F., Lince Klinger, F., 2009. Gravity characterization of the La Rioja Valley Basin, Argentina. Geophysics V74, 83–94 (Oklahoma; Año: 2009).
González Bonorino, F., 1950. Algunos problemas geológicos de las Sierras Pampean as. Rev. Asoc. Geol. Argent. 5 (3) (iil-110).
Götze, H.J., Krause, S., 2002. The Central Andean gravity high, a relic of an old subduction complex? J. S. Am. Earth Sci. 14, 799–811.
Grombein, T., Heck, B., Seitz, K., 2012. Optimized formulas for the gravitational field of a tesseroid. J. Geod. 87, 645-600.
Heck, B., Seitz, K., 2007. A comparison of the tesseroid, prism and point mass approaches for mass reductions in gravity field modeling. J. Geod. 81 (2), 121–136.
Introcaso, A., Martinez, M.P., Gimenez, M.E., 2000. Indicadores gavimétricos primarios de mecanismos isostáticos en cuencas sedimentarias. 20° Reunión Científica de la Asociación Argentina de Geofísicos y Geodestaspp. 187–189.
Introcaso, A., Martínez, M.P., Giménez, M.E., Ruiz, F., 2004. Gravi-magnetometric study of the Desaguadero Bermejo lineament separating Cuyania and Pampia terrains between 28° 45′ and 31° 30′South latitude. Gondwana Res. 7 (4), 117–1132.
Keller, M., Buggish, W., Lehnert, O., 1998. The stratigraphic record of the Argentine Precordillera and its plate tectonic background. Geol. Soc. Spec. Pub. 142 pp. 35–56 (London).
Kostadinoff, J., Bjerg, E.A., Delpino, S., Dimieri, L., Mogessie, A., Hoinkes, G., Hauzenberger, C.A., Felfernig, A., 1998. Gravimetric and magnetometric anomalies in the Sierras Pampeanas of San Luis. Rev. Asoc. Geol. Argent. 53, 549e552.
Kostadinoff, J., Bjerg, E.A., Gregori, D., Richarte, D., Robles, J.A., Raniolo, A., 2004. Geofísica del cuerpo ultramáfico de la mina Salamanca, provincia de Mendoza. Rev. Asoc. Geol. Argent. 59 (1) (Buenos Aires ene./mar. 2004).
Kostadinoff, J., Ferracutti, G.R., Bjerg, E.A., 2010. Interpretación de una Sección Gravimagnetométrica Sobre Pampa de las Invernadas. 67. Sierra Grande de San Luis Revista de la Asociación Geológica Argentina, Lugar: Buenos Aires, pp. 349–353.
Larrovere, M.A., de los Hoyos, C.R., Grosse, P., 2012. Los complejos metamórficos del retroarco Famatiniano (noroeste de Argentina): caracterización geoquímica e isotópica de sus protolitos e implicancias geotectónicas. Rev. Mexic. Ciencias Geol. 29 (3).
Limarino, C.O., Cesari, S.N., 1992. Reubicación estratigráfica de la Formación Cortaderas y definición del Grupo Angualasto (Carbonífero inferior, Precordillera de San Juan). Rev. Asoc. Geol. Argent. 47 (1), 61–72 (Buenos Aires).
Martinez, M.P., 1997. Tesis Doctoral inédita. Estudio del levantamiento de la Sierra de Valle Fértil. Universidad Nacional de Rosario. Facultad de Ciencias Exactas e Ingeniería, San Juan, Argentina.
Martínez, M.P., Giménez, M.E., 2003. Fuerte anomalía gravimétrica residual positiva en el Sistema de Famatina y su relación con paleo-suturas. Explicaciones alternativas. Rev. Asoc. Geol. Argent. 58, 176–186.
Miller, H., Söllner, F., 2005. The Famatinian complex (NW Argentina): back-docking of an island arc or terrane accretion? — Early Palaeozoic geodynamics at the western Gondwana margin. In: Vaughan, A.P.M., Leat, P.T., Pankhurst, R.J. (Eds.), Terrane Processes at the Margins of Gondwana. Geol. Soc. Lond. Spec. Publ. 246, pp. 241–256.
Mogessie, A., Hauzenberger, C.A., Hoinkes, G., Felfernig, A., Stumpfl, E.F., Bjerg, E.A., Kostadinoff, J., 2000. Genesis of platinum-group minerals in the Las Aguilas mafic–ultramafic rocks. Mineralogy and Petrology San Luis Province 68. Textural, Chemical and Mineralogical Evidence, Argentina, pp. 85–114.
Morelli, C., Gantar, C., Honkasalon, T., Mcconnel, K., Tanner, J.G., Szabo, B., Uotila, U., Whalen, C.T., 1974. The International Standardization Net 1971 (IGSN71). IUGG-IAG Publ. Spec. 4, Int. Union of Geod. And Geophys, Paris.
Otamendi, J., Ducea, M., Tibaldi, A., Bergantz, G., de La Rosa, J., Vujovich, G., 2009. Generation of tonalitic and dioritic magmas by coupled partial melting of gabbroic and metasedimentary rocks within the deep crust of the Famatinian magmatic arc. J. Petrol. 50, 841–873.
Otamendi, J.E., Ducea, M.N., Bergantz, G.W., 2012. Geological, petrological and geochemical evidence for progressive construction of an arc crustal section, Sierra de Valle Fértil, Famatinian arc, Argentina. J. Petrol. 53 (4) (761–800 pp.).
Pacino, M.C., Introcaso, A., 1987. Regional anomaly determination using the upwards—continuation method. Boll. Geofis. Teor. Appl. 29, 113–122.
Pail, R., Bruisma, S., Migliaccio, F., Förste, C., Goiginger, H., Schuh, W.D., Höck, E., Reguzzoni, M., Brockmann, J.M., Abrikosov, O., Veicherts, M., Fecher, T., Mayrhofer, R., Krasbutter, I., Sansò, F., Tscherning, C.C., 2011. First GOCE gravity field models derived by three different approaches. J. Geod. 85, 819–843.
Pankhurst, R.J., Rapela, C.W., Saavedra, J., Baldo, E., Dahlquist, J., Pascua, I., Fanning, C.M., 1998. The Famatinian magmatic arc in the central Sierras Pampeanas. In: En Pankhurst, R.J., Rapela, C.W. (Eds.), The Proto-Andean Margin of South America. Geol. Soc. Lond. Spec. Publ. 142, pp. 343–368.
Pankhurst, R.J., Rapela, C.W., Fanning, C.M., 2000. Age and origin of coeval TTG, I–S-type granites in the Famatinian belt of NW Argentina. Trans. R. Soc. Edinb. Earth Sci. 91, 151–168.
Pavlis, N.K., Holmes, S.A., Kenyon, S.C., Factor, J.K., 2008. An earth gravitational model to degree 2160. EGM08, Presented at the 2008 General Assembly of the European Geosciences Union, Vienna, Austria, April 13–18, 2008.
Pérez Luján, S.B., Ammirati, J.B., Alvarado, P., Vujovich, G., 2015s. Constraining a mafic thick crust model in the Andean Precordillera of the Pampean flat slab subduction region. J. S. Am. Earth Sci. http://dx.doi.org/10.1016/j.jsames.2015.09.005 (Article in Press).
Phillips, J.D., 2007. Geosoft executables (GX's). Developed by the U.S. Geological Survey, Version 2.0, with notes on GX Development from Fortran Code. Open File Report 2007-1355 (111 pp., Virginia).
Puranen, R., Elo, S., Airo, M.L., 1978. Areal and geological variation of rock densities, and their relation to some gravity anomalies in Finland. Geoskrifter. 10 p. 123e164 (Aarhus University).
Ramos, V.A., 1970. Estratigrafía y estructura del Terciario en la Sierra de los Colorados (Provincia de La Rioja), República Argentina. Rev. Asoc. Geol. Argent. 25 (3), 359–382.
Ramos, V.A., Jordan, T., Allmendinger, R.W., Kay, S.M., Cortés, J.M., Palma, M.A., 1984. Chilenia: un terreno alóctono en la evolución paleozoica de los Andes Centrales. IX Congreso Geológico Argentino. 2, p. 84e106.
Ramos, V.A., Jordan, T.E., Allmendinger, R.W., Mpodozis, C., Kay, S.M., Cortés, J.M., Palma, M.A., 1986. Paleozoic terranes of the Central Argentine–Chilean Andes. Tectonics 5, 855e880.
Ramos, V.A., Vujovich, G., Kay, S.M., Mcdonough, M.R., 1993. La orogénesis de Grenville en las Sierras Pampeanas Occidentales: la Sierra de Pie de Palo y su integración al supercontinente proterozoico. 12° Congreso Geológico Argentino y 2° Congreso de Exploración de Hidrocarburos, Actas 3, pp. 343–357 (Buenos Aires).
Ramos, V.A., Vujovich, G.I., Dallmeyer, R.D., 1996. Los klippes y ventanas tectónicas preándicas de la Sierra de Pie de Palo (San Juan): edad e implicaciones tectónicas. 13° Congreso Geológico Argentino y 3° Congreso de Exploración de Hidrocarburos (Mendoza), Actas 5, pp. 377–391 (Buenos Aires).
Ramos, V.A., Dallmeyer, R.D., Vujovich, G.I., 1998. Time constraints on the Early Paleozoic docking of the Precordillera, Central Argentina. In: Pankhurst, R.J., Rapela, C.W. (Eds.), The Proto-Andean Margin of Gondwana. Geol. Soc. Lond. Spec. Publ. 142 (143e158).
Ramos, V.A., 2004. Cuyania, an exotic block to Gondwana: review of a historical success and the present problems. Gondwana Res. 7, 1009–1026. http://dx.doi.org/10.1016/S1342-937X(05)71081-9.
Rapela, C.W., Pankhurst, R.J., Casquet, C., Baldo, E., Saavedra, J., Galindo, E., 1998. The Pampean orogeny of the southern proto-Andes evidence for Cambrian continental collision in the Sierras de Cordoba. In: Pankhurst, R.J., Rapela, C.W. (Eds.), The Proto-Andean Margin of South America. Geol. Soc. Lond., Spec. Publ. 142, pp. 182–217.
Rapela, C.W., Pankhurst, R., Baldo, E., Casquet, C., Galindo, C., Fanning, C., Saavedra, J., 2001. Ordovician metamorphism in the Sierras Pampeanas: new U–Pb SHRIMP ages in central-east Valle Fértil and the Velasco batholit. III South American Symposium on Isotopic Geology Pucón, Chile. Revista Comunicaciones, Santiago, pp. 616–619.
Ruiz, F., Introcaso, A., 2000. La estructura profunda de la cuenca sedimentaria Ischigualasto — Villa Unión: una interpretación tectónica a partir de datos de gravedad y magnetismo (Parte 1). UNR EditoraTemas de Geociencia N° 4 (70 pp. Rosario).
Ruiz, F., Luna, E., Vargas, D., Gimenez, M., Martinez, P., 2011. Importancia del ajuste y nivelación de datos aeromagnéticos a partir de magnetometría terrestre. Congreso Geológico Argentino. Neuquén. Actas en CD.
Sato, A.M., González, P.D., Llambías, E.L., 2003. Evolución del Orógeno Famatiniano en la Sierra de San Luis: magmatismo de arco deformación y metamorfismo de bajo a alto grado. Rev. Asoc. Geol. Argent. 58, 487–504.
Sims, J.P., Ireland, T.R., Camacho, A., Lyons, P., Pieters, P.E., Skirrow, R.G., Stuart-Smith, P.G., Miro, R., 2015. U–Pb, Th–Pb and Ar–Ar geochronology from the Southern Sierras Pampeanas. Argentina: Implications for the Palaeozoic Tectonic Evolution of the Western Gondwana Margin (in this volume).
Snyder, D., Ramos, V., Allmendinger, R., 1990. Thick-skinned deformation observed on deep seismic refection profiles in western Argentina. Tectonics 9, 773–788.
Thomas, W.A., Astini, R.A., 1996. The Argentine Precordillera: a traveler from the Ouachita embayment of North America Laurentia. Science 273, 752–757.
Thomas, W.A., Astini, R.A., 2003. Ordovician accretion of the Argentine Precordillera terrane to Gondwana: a review. J. S. Am. Earth Sci. 16, 667–679.
Toselli, A., Aceñolaza, F., RossideToselli, J., 1986. A proposal for the systematization of Upper Precambrian–Lower Palaeozoic basement in the Sierras Pampeanas, Argentina. Zbl. Geol. Paläontol. Teil I. Heft 9/10, 1227–1233 (Stuttgart).
Toselli, A.J., Saavedra, J., Rossi de Toselli, J.N., 1996. In: Aceñolaza, F.G., Miller, H., Toselli, A.J. (Eds.), Geología del Sistema de Famatina. Münchner Geologische Hefte A19, pp. 283–291.
Turner, J.C., 1962. Estratigrafía del tramo medio de la Sierra de Velazco y región al oeste, La Rioja. Bol. Acad. Nac. Cienc. 43, 5–54 (Córdoba).
Turner, J.C.M., 1964. Descripción geológica de la Hoja 15c, Vinchina (provincias de Catamarca y La Rioja). Dirección Nacional de Geología y Minería (81 p. Buenos Aires).
Uieda, L., Ussami, N., Braitenberg, C.F., 2010. Computation of the gravity gradient tensor due to topographic masses using tesseroids. Meet. Am. Suppl. Eos Trans. AGU 91(26) (Abstract G22A-04.http://code.google.com/p/tesseroids/).
Villar, L.M., 2003. Lavas almohadilladas del Cerro Chuscho. Provincia de La Rioja como parte de la ofiolita de la Precordillera Occidental. Correlaciones petrológicas en Cuyania y Chilenia. 10° Congreso Geológico Chileno.
Vujovich, G., 1992. Estudio petrológico y tectónico del metamorfismo de la sierra de La Huerta, provincia de San Juan Tesis Doctoral Universidad Nacional de La Plata (300 págs. (inédito). La Plata).
Vujovich, G.I., 1993. Arcos magmáticos islándicos en el sector occidental del terreno Pampeano. 12° Congreso Geológico Argentino y 2° Congreso Nacional de Hidrocarburos, Actas 4, pp. 17–22 (Buenos Aires).

Vujovich, G., Kay, S., 1996a. Evidencias geoquímicas del origen y ambiente geológico de las rocas metamórficas de composición máfica a intermedia de las Sierras Pampeanas Occidentales. 13° Congreso Geológico Argentino y 3° Congreso Nacional de Hidrocarburos, Actas 5, pp. 273–291 (Buenos Aires).

Vujovich, G., Kay, S., 1996b. Evidencias geoquímicas del origen y ambiente geológico de las rocas metamórficas de composición máfica a intermedia de las Sierras Pampeanas Occidentales [Geochemical evidence of the origin and geologic environment of the metamorphic rocks of mafic to intermediate composition of the Western Sierras Pampeanas]. 13° Congreso Geológico Argentino y 3° Congreso Nacional de Hidrocarburos, Actas 5, pp. 273–291.

Vujovich, G.I., Kay, S.M., 1998. A Laurentian? Grenville-age oceanic arc/back-arc terrane in the Sierra de Pie de Palo, Western Sierras Pampeanas, Argentina. In: Pankhrust, R.J., Rapela, C.W. (Eds.), The Proto-Andean Margin of Gondwana. Geol. Soc. Spec. Pub. 142, pp. 159–180 (Londres).

Weidmann, C., Spagnotto, S., Giménez, M., Martínez, P., Álvarez, O., Sánchez, M., Lince Klinger, F., 2013. Crustal structure and tectonic setting of the south Central Andes from gravimetric analysis. Geofis. Int. 52-3 pp. 197–208 (2013).

Zaffarana, C., Geuna, S., Poma, S., Patiño, Douce A., 2011. Reassessment of the volume of the Las Aguilas mafic–ultramafic intrusives, San Luis, Argentina, based on an alternative geophysical model. J. S. Am. Earth Sci. 32 (183-195).

Zapata, T.R., 1998. Crustal structure of the Andean thrust front at 30°S latitude from shallow and deep seismic reflection profiles, Argentina. J. S. Am. Earth Sci. 11 (2), 131–151.